Am J Transl Res 2022;14(1):264-274
www.ajtr.org /ISSN:1943-8141/AJTR0137542

Original Article

Gene expression analysis reveals immune and metabolic candidate pathways in the pathogenesis of chronic otitis media

Siran Lin[1], Wei Zhang[1], Yuzhen Xu[1], Qianqian Liu[1], Wenhong Zhang[1,2,3,4,5], Lingyun Shao[1,5]

[1]Department of Infectious Diseases, Huashan Hospital, [2]National Clinical Research Center for Aging and Medicine, Fudan University, Shanghai 200040, China; [3]Key Laboratory of Medical Molecular Virology (MOE/MOH) and Institutes of Biomedical Sciences, Shanghai Medical College, Fudan University, Shanghai 200032, China; [4]State Key Laboratory of Genetic Engineering, School of Life Science, Fudan University, Shanghai 200438, China; [5]Shanghai Key Laboratory of Infectious Diseases and Biosafety Emergency Response, Huashan Hospital, Fudan University, Shanghai 200438, China

Received July 20, 2021; Accepted November 9, 2021; Epub January 15, 2022; Published January 30, 2022

Abstract: Objectives: Chronic otitis media (COM) is a common disease and causes significant hearing impairment in many adults. Our study aimed to investigate the immune response in COM adult patients through RNA sequencing. Methods: In this study, we enrolled four adult COM patients and five healthy controls (HCs) to analyze and compare the mRNA signatures in their peripheral blood mononuclear cells (PBMCs). Gene Ontology functional enrichment and Kyoto Encyclopedia of Genes and Genomes pathway analyses were performed on the differentially expressed genes between the COM patients and the HCs. Furthermore, the immune cell proportions of the two groups were estimated by CIBERSORT. The GSE125532, GSE27990, and GSE23140 gene expression profiles were also retrieved and analyzed for comparison with our results. Results: Many immune pathways and genes were upregulated in the COM patients, including the IL-17 pathway and NLRP3. Monocytes and macrophages increased (P=0.005 and P=0.033, respectively), and the CD8+ T cells decreased (P=0.033) in the COM patients compared to the HCs. The COM patients' signatures also reflected a hypoxic state. Conclusions: Our findings emphasized the roles of several immune pathways and a hypoxic state in interpreting host responses during COM, and may enable the development of novel therapeutic tools for the disease.

Keywords: Chronic otitis media, differentially expressed genes, functional enrichment analysis, immune cell proportions, hypoxia

Introduction

Chronic otitis media (COM) is one of the leading causes of acquired hearing loss, particularly in developing countries [1]. Prevalence surveys showed that up to 330 million people suffer from it globally, 60% of whom had significant hearing impairment [1-3]. COM can have a significant adverse effect on the quality of life and cause life-threatening complications and mortality if left untreated [3].

COM is a disease characterized by chronic inflammation in the middle ear and mastoid cavity, with persistent or recurrent ear discharge through tympanic membrane perforation or the ventilation tube [4]. It usually results from improperly attended acute otitis media during childhood, and is also a sequela of secretory otitis media in some cases [5]. Individuals with COM could have middle ear effusion (MEE), that results in extracranial and intracranial complications persisting for years [5]. However, the pathogenesis of COM is still little understood. Thus, we aimed to investigate the immune response in adult COM patients through RNA sequencing (RNA-seq).

Materials and methods

Subjects

The samples were collected from adults diagnosed with COM at Huashan Hospital, Shanghai,

China. A total of four COM patients and five healthy controls (HCs) were included in the study. Three of the COM patients had a history of MEE for more than a year, and one had mastoid cholesteatoma. The HCs were recruited from age- and sex-matched healthy volunteers. All COM patients and HCs enrolled had no history of any current infectious or chronic disease and immunodeficiency, nor had received steroids or other immunomodulatory agents. The demographic and clinical data of the COM patients were collected.

Sample collection and RNA isolation

Peripheral blood mononuclear cells (PBMCs) were isolated from peripheral venous blood by Ficoll density gradient centrifugation (Cedarlane, Burlington, Canada). Then, total RNA was extracted from the PBMCs using Trizol reagent (Ambion, Carlsbad, CA, USA). RNA purity and concentration were evaluated using a NanoDrop and Agilent 2100 Bioanalyzer (Thermo Fisher Scientific, MA, USA).

RNA-Seq and analysis

mRNA was purified and enriched by Oligo(dT)-attached magnetic beads. The RNA-seq libraries were performed by the Beijing Genomics Institute (BGI) in Shenzhen, China. The mRNA was fragmented into 200-bp short fragments and reverse transcribed to cDNA with random hexamer primers. The final library was amplified with phi29 to make DNA nanoballs (DNBs), which have more than 300 copies of one molecule. DNBs were loaded into the patterned nanoarray, and single-end 50-base reads were generated on the BGIseq500 platform (BGI-Shenzhen, China).

The raw read counts for gene expression were quantified using SOAPnuke v1.5.2 [6] based on the adapter contamination and the average base read quality to obtain high-quality clean reads. The low-quality reads, including the adaptor sequences, those with >20% bases with a quality score of <10, and those with >5% ambiguous bases (N bases), were removed from the sequencing data using the trimmomatic v0.36 [7]. The clean data were then aligned against GCF_000001405.37_GRCh38.p11 (NCBI) using HISAT2 v2.0.4 [8] and Bowtie2 v2.2.5 [9]. The RSEM v1.2.12 software was used to estimate the read counts and the FPKM (fragments per kilobase of transcript per million fragments mapped) values at the gene level [10]. The significance and fold change of differentially expressed genes (DEGs) between COM and HCs were estimated using the DESeq2 [11] method. Genes with false discovery rate (FDR) <0.05 and log2 |fold change| >1.5 were considered as significant DEGs.

Gene clustering and pathway analysis

Expression data of DEGs were visualized using the R package *heatmap*. To further compare gene expression levels between the two groups, volcano plots were generated using the R package *ggplot2*. The Gene ontology (GO) and Kyoto Encyclopedia of Genes and Genomes (KEGG) analyses for DEGs were performed using the package *clusterProfile*r [12] with *P*-value <0.05 set as the threshold value. The *plots* and *cowplot* R packages were used for data visualization.

The CIBERSORT [13] online tool was used to estimate the abundances of immune cell types, based on gene FPKM values. The cell abundances of the two groups were then compared using unpaired Student's t-test. The statistical tests were performed using GraphPad Prism (version 8.0.2) for Windows (GraphPad Software, San Diego, CA, USA) and statistical significance was set at P<0.05.

GSE125532, GSE27990 [14], and GSE23140 [15] datasets were downloaded from the GEO database (http://www.ncbi.nlm.nih.gov/geo/) and were analyzed as described above.

Results

Transcriptome responses in adults with COM

The clinical and demographic characteristics of the COM patients are provided in **Table 1**. Out of 19339 genes assessed, 1183 (6.1%) were differentially expressed by at least 1.5 for log2 |fold change|, whether up- or downregulated, between the COM patients and the HCs (FDR<0.05). The expression data of these genes were used to perform K-means clustering, which revealed that the COM patients had unique expression profiles compared to HCs (**Figure 1A**). Of these DEGs, 1076 transcripts (91.0% overall) were upregulated in the COM patients, while only 107 (9.0%) were downregu-

Table 1. Clinical and demographic characteristics of the COM patients

COM patient no.	Age (years)	Gender	Diagnosis	Complication	Blood routine	CRP (mg/L) ESR (mm/h) PCT (ng/ml)
1	61	Male	Chronic suppurative otitis media in the right ear	Bilateral sensorineural hearing loss; Right mastoiditis; Right facial nerve palsy	WCC: 9.87 * 10^9/L; N: 93.3%; HGB: 159 g/L; PLT: 308 * 10^9/L	<3.03; 8; 0.02
2	64	Male	Chronic suppurative otitis media in the right ear	NA	WCC: 3.83 * 10^9/L; N: 61.6%; HGB: 135 g/L; PLT: 297 * 10^9/L	<3.03; 33; 0.05
3	26	Female	Chronic otitis media in the left ear	Left mastoid cholesteatoma; Cerebellar abscess	WCC: 25.79 * 10^9/L; N: 88%; HGB: 151 g/L; PLT: 433 * 10^9/L	146; 38; 0.43
4	52	Female	Chronic suppurative otitis media in the left and right ear	Suppurated meningitis	WCC: 8.66 * 10^9/L; N: 82.2%; HGB: 128 g/L; PLT: 285 * 10^9/L	<3.03; 2; 0.03

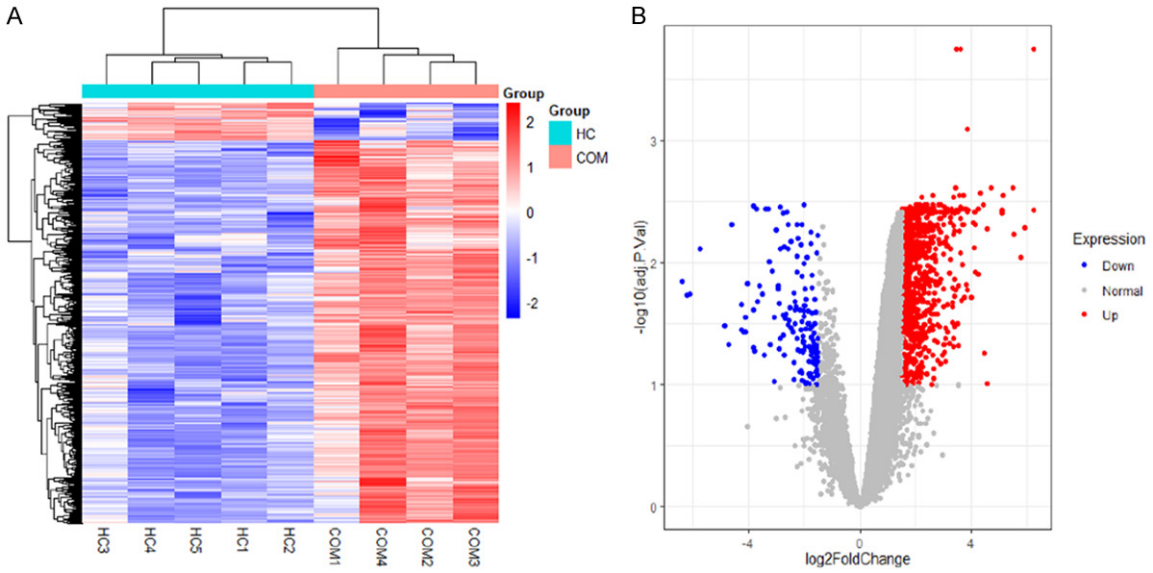

Figure 1. Heatmap and volcano plot of DEGs in PBMC between the COM patients and HCs. A. Heatmap of the 1076 upregulated DEGs and 107 downregulated DEGs. B. Upregulated (red dots) and downregulated (blue dots) DEGs and normally expressed genes (gray dots) showed in the volcano plot.

lated (**Figure 1B**). The top 20 up- and downregulated DEGs are listed in **Table 2**.

Pathways significantly enriched in patients with COM

GO and KEGG analyses were done for pathway classification of the DEGs between the COM patients and HCs. For the upregulated DEGs, the top three enriched biologic processes were response to the molecule, regulation of hematopoiesis, and response to lipopolysaccharide (**Figure 2A**). The top three terms in cellular components were specific granule, protein-DNA complex, and nucleosome (**Figure 2B**). No molecular function terms were enriched with the upregulated DEGs. On the other hand, the GO terms enriched by the downregulated DEGs were predominantly associated with cellular respiration and energy metabolism. These pathways are critical for necessary cellular activities and survival, and include oxygen transport, gas transport, oxygen carrier activity, and oxygen binding (**Figure 2C-E**). The top ten enriched GO terms of up- and downregulated DEGs are shown in **Tables 3** and **4**, respectively.

As shown in the gene interaction network based on enriched GO terms (**Figure 2F** and **2G**), the main pathways enriched by upregulated DEGs were cellular response to biotic stimulus,

Table 2. Top 20 upregulated and downregulated DEGs

Gene symbol	Log2FoldChange	*P* value	adj.*P.val*	Gene description
Upregulated				
HIST1H1D	6.252028648	2.41E-05	0.003656431	Histone H1.3
ID1	6.227290692	3.51E-08	0.000174923	DNA-binding protein inhibitor ID-1
HIST1H1E	5.935040861	0.000152324	0.00511242	Histone H1.4
SLC12A1	5.790734808	0.000721145	0.009056062	Solute carrier family 12 member 1
HIST2H2AB	5.534473563	0.000235769	0.005835844	Histone H2A type 2-B
NR4A3	5.479935189	9.44E-07	0.002419085	Nuclear receptor subfamily 4 group A member 3
HIST1H1B	5.14821594	2.17E-06	0.002811706	Histone H1.5
IER3	5.105063681	4.84E-05	0.003915135	Immediate early response 3
FOSB	5.094659181	2.34E-05	0.003656431	FosB Proto-Oncogene, AP-1 transcription factor submit
JUN	4.71864414	1.13E-06	0.002419085	Jun Proto-Oncogene, AP-1 transcription factor subunit
LOC105376875	4.555533216	0.000174326	0.005301115	NA
FOSL1	4.442650148	4.73E-06	0.003337417	FOS Like 1, AP-1 Transcription Factor Subunit
PHLDA2	4.315972771	1.42E-06	0.002664335	Pleckstrin Homology Like Domain Family A Member 2
MINDY4B	4.25958578	0.001230787	0.012378962	NA
LOC107985678	4.259096659	1.89E-05	0.003575597	NA
NFKBIA	4.156564575	9.61E-05	0.004818302	NF-Kappa-B Inhibitor Alpha
ADAMTS2	4.156502522	0.001138192	0.01185095	A Disintegrin-Like And Metalloprotease (Reprolysin Type) With Thrombospondin Type 1 Motif 2
SNAI1	4.156238712	3.50E-05	0.003815902	Snail Family Transcriptional Repressor 1
AREG	4.119979414	0.000468867	0.007511613	Amphiregulin
C4orf47	4.117414056	3.54E-05	0.003815902	Chromosome 4 Open Reading Frame 47
Downregulated				
HBA2	-6.395749772	0.001548036	0.014330585	Hemoglobin Subunit Alpha 2
HBB	-6.204116376	0.002317303	0.018470559	Hemoglobin Subunit Beta
HBA1	-6.102545011	0.002265	0.018140603	Hemoglobin Subunit Alpha 1
HBG2	-5.759256519	0.000486763	0.007644862	Hemoglobin Subunit Gamma 2
HBM	-4.846516929	0.00565453	0.032769128	Hemoglobin Subunit Mu
ALAS2	-4.723757191	0.009552469	0.0467987	5'-Aminolevulinate Synthase 2
NEDD8-MDP1	-4.597716621	9.70E-05	0.004818302	NEDD8-MDP1 Readthrough
HBG1	-4.249049174	0.003036941	0.021876788	Hemoglobin Subunit Gamma 1
AHSP	-4.244347264	0.006338473	0.035317613	Alpha Hemoglobin Stabilizing Protein
HBD	-4.186873344	0.006707026	0.036673334	Hemoglobin Subunit Delta
HBZ	-4.111712262	0.006690925	0.03663367	Hemoglobin Subunit Zeta
EPB42	-4.09994924	0.004409725	0.027781638	Erythrocyte Membrane Protein Band 4.2
MYOM2	-4.054531909	0.001631104	0.014766764	Myomesin 2
SELENBP1	-3.839757799	0.010361638	0.049422038	Selenium Binding Protein 1
VWCE	-3.829684576	0.003529286	0.024128796	Von Willebrand Factor C And EGF Domains
PLVAP	-3.812947776	5.71E-06	0.003419133	Plasmalemma Vesicle Associated Protein
KLC3	-3.72968654	1.08E-05	0.003575597	Kinesin Light Chain 3
CX3CR1	-3.689442748	0.002776437	0.020707763	C-X3-C Motif Chemokine Receptor 1
TCL1A	-3.610056147	0.001745886	0.015327959	T Cell Leukemia/Lymphoma 1A
KLF1	-3.520515514	0.002253333	0.018100767	Kruppel Like Factor 1

response to molecule of bacterial origin, response to lipopolysaccharide, regulation of MAP kinase activity, and p38 MAPK cascade. The upregulated genes were predominately associated with the immune response, especially the innate immune response. The upregulated expression of *MPO*, *ELANE*, *LCN2*, and *CXCL2* suggest neutrophils are activated in COM patients. *IL-10* and *ARG1* are biomarkers of alternatively activated macrophages, and the latter indicates an anti-inflammatory response of macrophages. The upregulation of

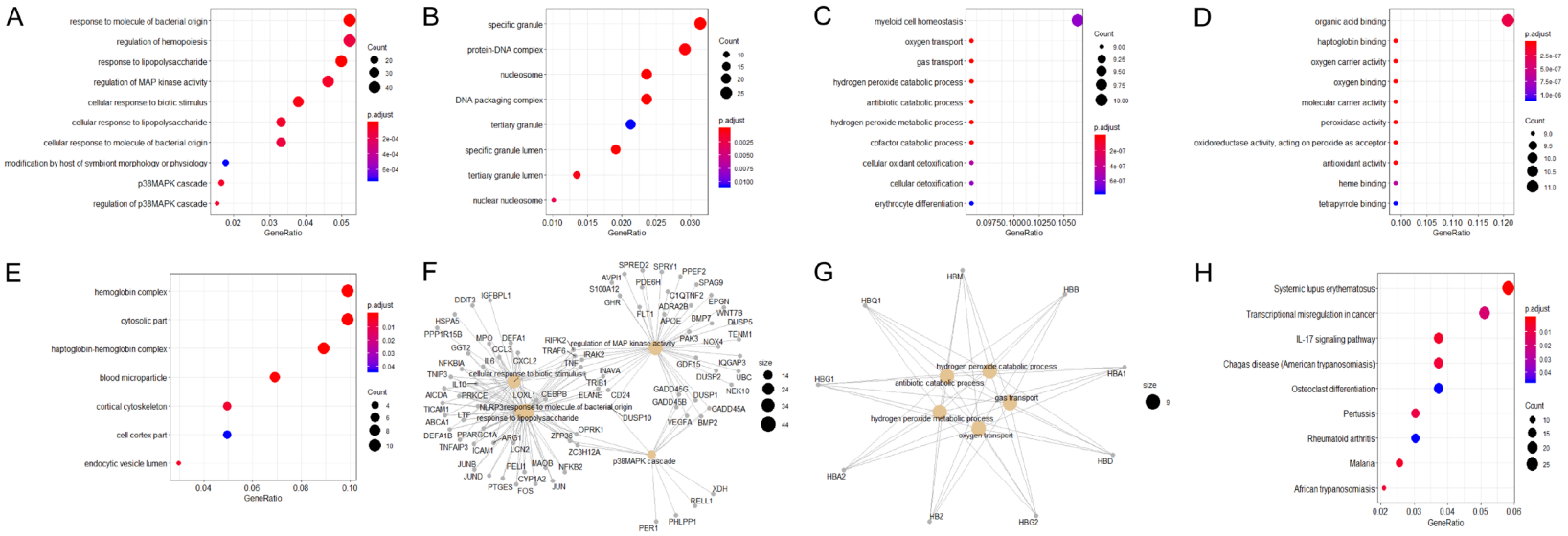

Figure 2. Functional enrichment analysis of DEGs in COM patients. A, B. Biological process and cellular component GO terms enriched in upregulated DEGs. C-E. Biological process, molecular function, and cellular component GO terms enriched in downregulated DEGs. F, G. Gene-concept networks based on enriched GO terms. H. KEGG enrichment analysis.

Table 3. Top 10 enriched GO terms of upregulated DEGs

ID	Term	*P*-value
GO:0002237	response to molecule of bacterial origin	3.305613e-10
GO:0032496	response to lipopolysaccharide	1.045679e-09
GO:0071216	cellular response to biotic stimulus	1.694886e-08
GO:0038066	p38MAPK cascade	5.355668e-08
GO:0043405	regulation of MAP kinase activity	8.129895e-08
GO:1900744	regulation of p38MAPK cascade	8.531626e-08
GO:0071222	cellular response to lipopolysaccharide	1.138968e-07
GO:1903706	regulation of hemopoiesis	2.274575e-07
GO:0071219	cellular response to molecule of bacterial origin	2.374900e-07
GO:0051851	modification by a host of symbiont morphology or physiology	1.439005e-06

Table 4. Top 10 enriched GO terms of downregulated DEGs

ID	Term	*P*-value
GO:0015671	oxygen transport	7.463613e-18
GO:0015669	gas transport	1.354904e-16
GO:0042744	hydrogen peroxide catabolic process	3.897955e-14
GO:0017001	antibiotic catabolic process	1.127081e-11
GO:0042743	hydrogen peroxide metabolic process	1.127081e-11
GO:0051187	cofactor catabolic process	5.898414e-11
GO:0098869	cellular oxidant detoxification	2.179699e-09
GO:1990748	cellular detoxification	3.084910e-09
GO:0002262	myeloid cell homeostasis	3.540949e-09
GO:0030218	erythrocyte differentiation	5.059769e-09

NLRP3 suggests that the inflammasome could also be involved in the pathophysiology of COM. The genes in the downregulated network all come from the hemoglobin submit family, suggesting a hypoxic state in the COM patients compared with HCs.

A total of nine signaling pathways were enriched in the KEGG pathway analysis, seven of which were associated with the upregulated DEGs and two with the downregulated DEGs (**Figure 2H**). The IL-17 signaling pathway was enriched and upregulated, with the following genes involved: *FOSB*, *JUN*, *FOSL*, *NFKBIA*, *CXCL2*, *TNFAIP3*, *LCN2*, *FOS*, *JUND*, *TNF*, *CEBPB*, *IFNG*, *MAPK6*, *IL6*, *MAPK12* and *TRAF6*.

GO and KEGG analysis of existing GEO datasets of patients with COM

We downloaded the GSE125532 dataset from the NCBI GEO DataSets that had whole blood and middle ear excretion transcriptome information of 11 pediatric COM patients with mucoid or serous excretion. The transcriptomes of excretion could furthermore reveal the local inflammatory reaction and metabolism characteristics in the middle ear. We analyzed the DEGs of the whole blood compared with the mucoid (**Figures 3**, and **4**) or serous (Supplementary Figures 1, and 2) excretion. The differences were similar regardless of the nature of the discharge.

The top ten enriched GO terms in three aspects are shown in **Figure 3**. The results of the GO enrichment in the biologic process were close to ours, with the neutrophil activation pathway upregulated and T cell activation pathway downregulated in the excretion samples. In molecular function, the oxygen carrier activity pathway was enriched and downregulated. Both KEGG analyses showed upregulation of the PPAR and the Toll-like receptor signaling pathways (**Figure 4**). On the contrary, the Natural killer-mediated cytotoxicity, T cell receptor signaling pathway, Th1 and Th2 cell differentiation, Th17 cell differentiation, and NF-kappa B signaling pathway were downregulated in both KEGG results (**Figure 4**).

Abundances of immune cell types were different in patients with COM, acute otitis media, and controls (HCs)

We estimated the proportions of 22 types of the immune cells in our PBMC samples by analyzing our gene expression dataset with the online tool CIBERSORT. The result showed that the levels of monocytes and macrophages were predicted to be significantly higher (P=0.005 and P=0.033, respectively) and CD8+ T cells

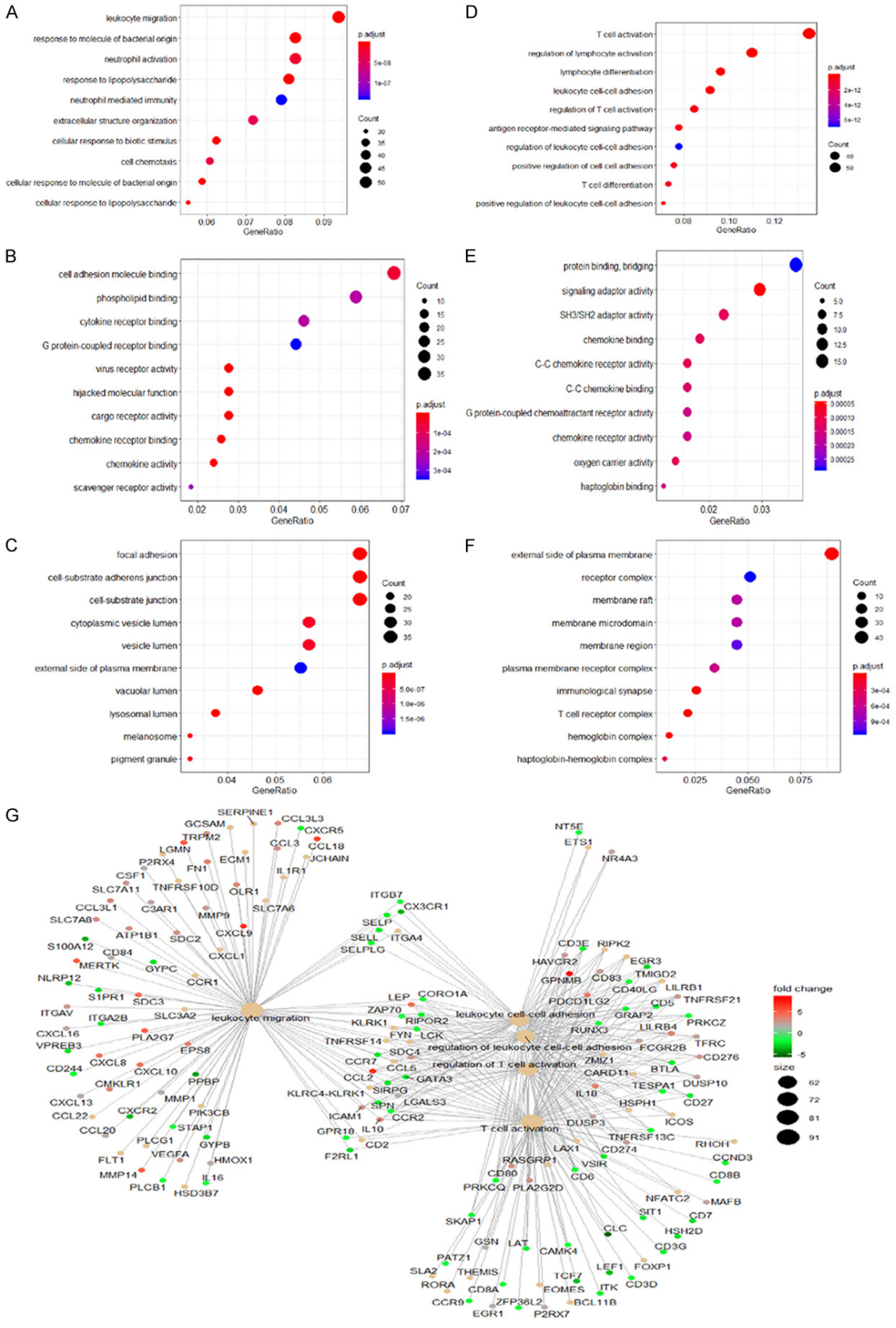
A
leukocyte migration
response to molecule of bacterial origin
neutrophil activation
response to lipopolysaccharide
neutrophil mediated immunity
extracellular structure organization
cellular response to biotic stimulus
cell chemotaxis
cellular response to molecule of bacterial origin
cellular response to lipopolysaccharide
p.adjust
Count
GeneRatio
B
cell adhesion molecule binding
phospholipid binding
cytokine receptor binding
G protein-coupled receptor binding
virus receptor activity
hijacked molecular function
cargo receptor activity
chemokine receptor binding
chemokine activity
scavenger receptor activity
C
focal adhesion
cell-substrate adherens junction
cell-substrate junction
cytoplasmic vesicle lumen
vesicle lumen
external side of plasma membrane
vacuolar lumen
lysosomal lumen
melanosome
pigment granule
D
T cell activation
regulation of lymphocyte activation
lymphocyte differentiation
leukocyte cell-cell adhesion
regulation of T cell activation
antigen receptor-mediated signaling pathway
regulation of leukocyte cell-cell adhesion
positive regulation of cell-cell adhesion
T cell differentiation
positive regulation of leukocyte cell-cell adhesion
E
protein binding, bridging
signaling adaptor activity
SH3/SH2 adaptor activity
chemokine binding
C-C chemokine receptor activity
C-C chemokine binding
G protein-coupled chemoattractant receptor activity
chemokine receptor activity
oxygen carrier activity
haptoglobin binding
F
external side of plasma membrane
receptor complex
membrane raft
membrane microdomain
membrane region
plasma membrane receptor complex
immunological synapse
T cell receptor complex
hemoglobin complex
haptoglobin-hemoglobin complex
G
leukocyte migration
leukocyte cell-cell adhesion
regulation of leukocyte cell-cell adhesion
regulation of T cell activation
T cell activation
fold change
size

Figure 3. Functional enrichment analysis of DEGs in mucoid excretion samples of GSE125532. A-C. Biological process, molecular function, and cellular component GO terms enriched in upregulated DEGs. D-F. Biological process, molecular function, and cellular component GO terms enriched in downregulated DEGs. G. Gene-concept networks based on enriched GO terms.

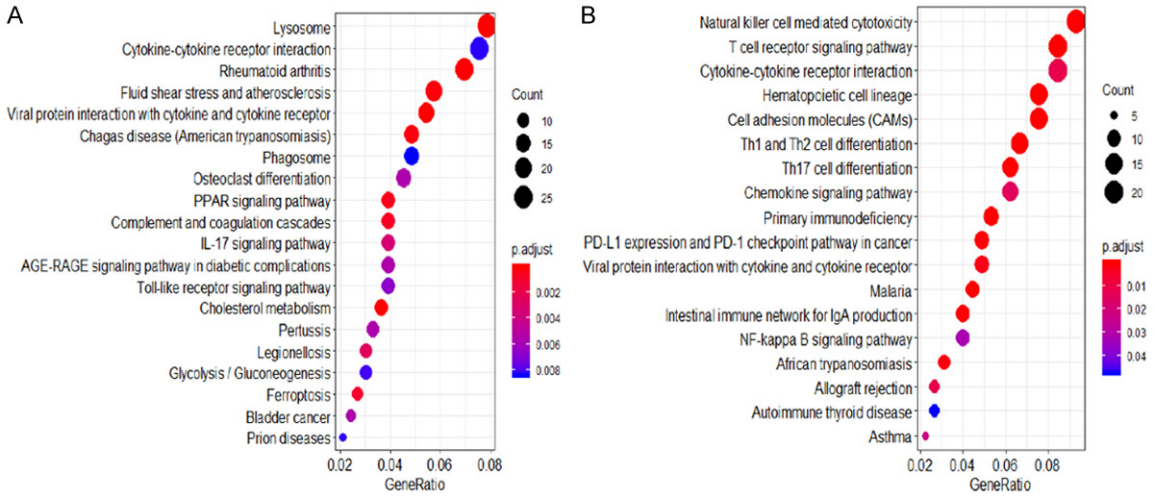

Figure 4. KEGG enrichment analysis of DEGs in mucoid excretion samples of GSE125532. A. Upregulated. B. Downregulated.

were lower (P=0.033) in the COM patients than in the HCs (**Figure 5A**). The differences of monocytes and CD8+ T cells were further validated in clinic samples, and the result of monocytes was consistent with CIBERSORT (Supplementary Figure 5).

Furthermore, we also analyzed the GSE125532 dataset with CIBERSORT to validate our results. The mucoid secretion samples had higher levels of memory B cells and macrophages M0, M1, and M2 compared to the whole blood samples (P=0.015, P=0.002, P=0.015, and P=0.002, respectively) (Supplementary Figure 3). Likewise, the proportions of naïve B cells, CD8-positive T cells, CD4 naïve T cells, resting NK cells, and monocytes were lower (P=0.002, P=0.002, P=0.0004, P=0.0006 and P=0.021, respectively) (**Figure 5B**). The same results could be seen in the serous secretion samples compared with their paired whole blood samples (Supplementary Figure 4). Besides, there were fewer activated memory CD4 positive T cells and more neutrophils in whole blood samples compared with serous secretion samples (P=0.023 and P≤0.0001, respectively) (**Figure 5C**).

To show the differences in immune response for acute otitis media (AOM) and COM, gene expression in the datasets GSE23140 and GSE27990 were also analyzed. In both datasets, there were four AOM children's whole blood transcriptome data at two time points: before and after the onset of AOM. As the results of CIBERSORT showed, no significant difference in the proportions of immune cells was found in these children after they developed AOM.

Discussion

COM is a common disease, which is classified into the squamous or mucosal type and may be active or inactive. Its pathogenesis is multifactorial with both genetic and environmental factors involved, as well as the anatomic and functional characteristics of the Eustachian tube. In this study, we enrolled four adult patients with COM to explore their transcriptome characteristics and to identify host immune factors involved in the pathogenesis of COM.

In our results, the IL-17 signaling pathway and one of its downstream signaling activities, MAP kinase activity, were upregulated, suggesting IL-17 signaling might play a role in response to middle ear inflammation. However, pathways involved in the differentiation of IL-17A-producing CD4+ cells such as Th17 cell differentiation and NF-kappa B signaling pathway were downregulated in excretion samples of

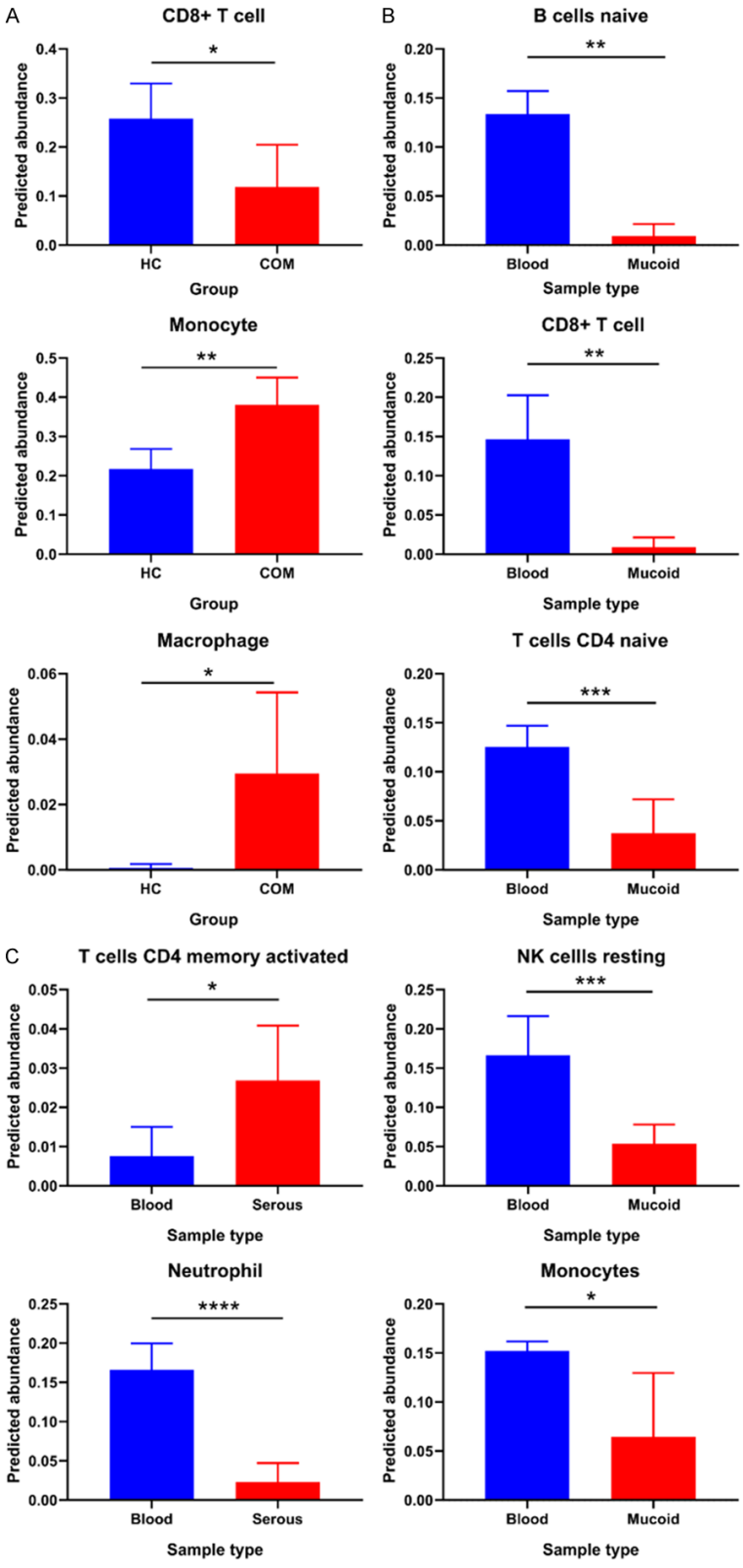

Figure 5. FPKM based CIBERSORT predicted blood cell abundance between COM patients and HCs, and between different sample types. Data are mean ± SE. *P<0.05, **P<0.01, ***P<0.001.

GSE125532, contrary to ours. A dysregulated IL-17 signaling pathway can cause excessive pro-inflammatory cytokine expression and chronic inflammation, particularly at mucosal sites [16, 17]. Previous studies have shown an elevated level of IL-17 in both serum and middle ear fluid of children with otitis media with effusion [18, 19]. It was also observed in IL-17A knockout mouse models that IL-17A could promote the production of MPO by p38 MAPK signaling pathway, which is associated with middle ear tissue injury [20]. Furthermore, IL-17 expression was shown to be increased in patients with chronic sinusitis, which usually co-occurred with COM [21]. These findings demonstrated the contribution of IL-17 signaling in the pathogenesis of COM.

Toll-like receptors (TLRs) and Nod-like receptors (NLRs) were both subsets of pattern-recognition receptors (PRRs). The importance of TLRs in human middle ear inflammation had already been described in previous studies and likewise shown in our analysis (**Figure 4**). Interestingly, one of the NLRs, the nucleotide-binding oligomerization domain-like receptor protein 3 (NLRP3), was also upregulated. The NLRP3 inflammasome is a critical molecule mediating IL-1β and IL-18 responses. NLRP3 was observed to be induced by the transtympanic injection of lipopolysaccharide in mouse models [22] and was significantly elevated in the middle ear tissue of COM patients [23].

The neutrophil activation pathway was found to be upregulated in COM patients, especially in the excretion sample, with upregulated expression of *MPO*, *ELANE*, *LCN2*, and *CXCL2*. The activation of neutrophils in the middle ear may be related to the chronicity and recurrence of otitis media. As shown in previous studies, the neutrophil extracellular traps (NETs), together with persistent Nontypeable *Haemophilus influenzae* (NTHi) populations, were found to be within the biofilms in the middle ear chamber of COM patients [24-26]. Moreover, NTHi was able to survive within the NETs and resist killing of the host immune system, and NETs were thought to be responsible for the bacterial persistence in the middle ear [27].

Cell-mediated immune responses to COM are poorly understood, and currently published studies contradictory. NTHi and *Staphylococcus aureus* are the most common pathogens of AOM and COM [28]. As shown in an NTHi infection OME mouse model, neutrophil and macrophage numbers were increased in both blood and spleen after infection [29]. Otitis-prone children had more circulating NK cells and CD8+ T cells than HCs, suggesting otitis-prone children did not have impaired cell-mediated immunity [30]. Besides, the levels of peripheral blood CD4+ and CD8+ lymphocytes levels were showed to increase in children with OME [31].

The gene interaction network of downregulated DEGs revealed that pathways of oxygen transport, hydrogen peroxide metabolic process, and hydrogen peroxide catabolic process were inhibited, suggesting hypoxia might play an essential role in COM. Earlier studies that had shown hypoxia in the middle ear cavity was associated with local inflammation and the production of effusion. Besides, the therapeutic effect of inhibiting hypoxia by surgical ventilation had previously been evaluated with optimistic results achieved [32]. However, in addition to local hypoxia in the middle ear cavity, our results revealed COM patients were in a whole-body hypoxic state compared to HCs.

In conclusion, unbalanced innate immune response and hypoxia were likely to be of great significance in the pathogenesis of COM. However, questions remain, and further studies are needed to explore the specific roles of the different kinds of immune cells in COM patients and the potential relationship between hypoxia and COM.

Acknowledgements

This work was supported by the Key Laboratory Project of Shanghai Science and Technology Commission [grant numbers 20dz2210400].

Disclosure of conflict of interest

None.

Address correspondence to: Dr. Lingyun Shao, Department of Infectious Diseases, Huashan Hospital, Fudan University, 12 Wulumuqi Zhong Road, Shanghai 200040, China. Tel: +86-21-52888262; Fax: +86-21-52888262; E-mail: lingyun26@fudan.edu.cn

References

[1] Acuin J. Chronic suppurative otitis media: burden of illness and management options. Geneve World Health Organization 2004.

[2] Abraham ZS, Ntunaguzi D, Kahinga AA, Mapondella KB, Massawe ER, Nkuwi EJ and Nkya A. Prevalence and etiological agents for chronic suppurative otitis media in a tertiary hospital in Tanzania. BMC Res Notes 2019; 12: 429.

[3] Monasta L, Ronfani L, Marchetti F, Montico M, Vecchi Brumatti L, Bavcar A, Grasso D, Barbiero C and Tamburlini G. Burden of disease caused by otitis media: systematic review and global estimates. PLoS One 2012; 7: e36226.

[4] Schilder AG, Chonmaitree T, Cripps AW, Rosenfeld RM, Casselbrant ML, Haggard MP and Venekamp RP. Otitis media. Nat Rev Dis Primers 2016; 2: 16063.

[5] Wallis S, Atkinson H and Coatesworth AP. Chronic otitis media. Postgrad Med 2015; 127: 391-395.

[6] Chen Y, Chen Y, Shi C, Huang Z, Zhang Y, Li S, Li Y, Ye J, Yu C, Li Z, Zhang X, Wang J, Yang H, Fang L and Chen Q. SOAPnuke: a MapReduce acceleration-supported software for integrated quality control and preprocessing of high-throughput sequencing data. Gigascience 2018; 7: 1-6.

[7] Bolger AM, Lohse M and Usadel B. Trimmomatic: a flexible trimmer for Illumina sequence data. Bioinformatics 2014; 30: 2114-2120.

[8] Kim D, Langmead B and Salzberg SL. HISAT: a fast spliced aligner with low memory requirements. Nat Methods 2015; 12: 357-360.

[9] Langmead B and Salzberg SL. Fast gapped-read alignment with bowtie 2. Nat Methods 2012; 9: 357-359.

[10] Li B and Dewey CN. RSEM: accurate transcript quantification from RNA-Seq data with or without a reference genome. BMC Bioinformatics 2011; 12: 323.
[11] Love MI, Huber W and Anders S. Moderated estimation of fold change and dispersion for RNA-seq data with DESeq2. Genome Biol 2014; 15: 550.
[12] Yu G, Wang LG, Han Y and He QY. clusterProfiler: an R package for comparing biological themes among gene clusters. OMICS 2012; 16: 284-287.
[13] Newman AM, Liu CL, Green MR, Gentles AJ, Feng W, Xu Y, Hoang CD, Diehn M and Alizadeh AA. Robust enumeration of cell subsets from tissue expression profiles. Nat Methods 2015; 12: 453-457.
[14] Liu K, Chen L, Kaur R and Pichichero ME. Transcriptome signature in young children with acute otitis media due to non-typeable Haemophilus influenzae. Int Immunol 2013; 25: 353-361.
[15] Liu K, Chen L, Kaur R and Pichichero M. Transcriptome signature in young children with acute otitis media due to streptococcus pneumoniae. Microbes Infect 2012; 14: 600-609.
[16] Isailovic N, Daigo K, Mantovani A and Selmi C. Interleukin-17 and innate immunity in infections and chronic inflammation. J Autoimmun 2015; 60: 1-11.
[17] Jin W and Dong C. IL-17 cytokines in immunity and inflammation. Emerg Microbes Infect 2013; 2: e60.
[18] Kwon OE, Park SH, Kim SS, Shim HS, Kim MG, Kim YI, Kim SH and Yeo SG. Increased IL-17 and 22 mRNA expression in pediatric patients with otitis media with effusion. Int J Pediatr Otorhinolaryngol 2016; 90: 188-192.
[19] Yeghaneh Moghaddam A, Talaei R, Nikoueinejad H and Akbari H. Studying the serum as well as serous level of IL-17 and IL-23 in patients with serous otitis media. Iran J Allergy Asthma Immunol 2017; 16: 520-524.
[20] Wang W, Liu W, Liu J, Wang Z, Fan F, Ma Y, Jin C, Xiang Y, Huang Y, Zhang X, Xu W, Yin Y and He Y. Interleukin-17A aggravates middle ear injury induced by streptococcus pneumoniae through the p38 mitogen-activated protein kinase signaling pathway. Infect Immun 2017; 85:
[21] Hu XD, Bao YY, Zhou SH, Yao HT, Mao JY, Ji XX and Wu XH. Interleukin-17A expression in patients with chronic rhinosinusitis and its relationship with clinical features. J Int Med Res 2013; 41: 777-784.
[22] Kariya S, Okano M, Zhao P, Maeda Y, Kataoka Y, Higaki T, Noda Y, Makihara S and Nishizaki K. NLRP3 inflammasome expression in lipopolysaccharide-induced otitis media. Acta Otolaryngol 2018; 138: 1061-1065.
[23] Kariya S, Okano M, Zhao P, Kataoka Y, Yoshinobu J, Maeda Y, Ishihara H, Higaki T and Nishizaki K. Activation of NLRP3 inflammasome in human middle ear cholesteatoma and chronic otitis media. Acta Otolaryngol 2016; 136: 136-140.
[24] Hall-Stoodley L, Hu FZ, Gieseke A, Nistico L, Nguyen D, Hayes J, Forbes M, Greenberg DP, Dice B, Burrows A, Wackym PA, Stoodley P, Post JC, Ehrlich GD and Kerschner JE. Direct detection of bacterial biofilms on the middle-ear mucosa of children with chronic otitis media. JAMA 2006; 296: 202-211.
[25] Hong W, Juneau RA, Pang B and Swords WE. Survival of bacterial biofilms within neutrophil extracellular traps promotes nontypeable haemophilus influenzae persistence in the chinchilla model for otitis media. J Innate Immun 2009; 1: 215-224.
[26] Val S, Poley M, Brown K, Choi R, Jeong S, Colberg-Poley A, Rose MC, Panchapakesan KC, Devaney JC, Perez-Losada M and Preciado D. Proteomic characterization of middle ear fluid confirms neutrophil extracellular traps as a predominant innate immune response in chronic otitis media. PLoS One 2016; 11: e0152865.
[27] Juneau RA, Pang B, Weimer KE, Armbruster CE and Swords WE. Nontypeable haemophilus influenzae initiates formation of neutrophil extracellular traps. Infect Immun 2011; 79: 431-438.
[28] Ngo CC, Massa HM, Thornton RB and Cripps AW. Predominant bacteria detected from the middle ear fluid of children experiencing otitis media: a systematic review. PLoS One 2016; 11: e0150949.
[29] Vikhe PP, Purnell T, Brown SDM and Hood DW. Cellular immune response against nontypeable haemophilus influenzae infecting the pre-inflamed middle ear of the junbo mouse. Infect Immun 2019; 87: e00689-19.
[30] Seppanen E, Tan D, Corscadden KJ, Currie AJ, Richmond PC, Thornton RB and Kirkham LS. Evidence of functional cell-mediated immune responses to nontypeable haemophilus influenzae in otitis-prone children. PLoS One 2018; 13: e0193962.
[31] Fan W, Li X, Xu H, Zhao L, Zhao J and Li W. Relationship of T lymphocytes, cytokines, immunoglobulin E and nitric oxide with otitis media with effusion in children and their clinical significances. Rev Assoc Med Bras (1992) 2019; 65: 971-976.
[32] Bhutta MF, Cheeseman MT and Brown SD. Myringotomy in the Junbo mouse model of chronic otitis media alleviates inflammation and cellular hypoxia. Laryngoscope 2014; 124: E377-383.

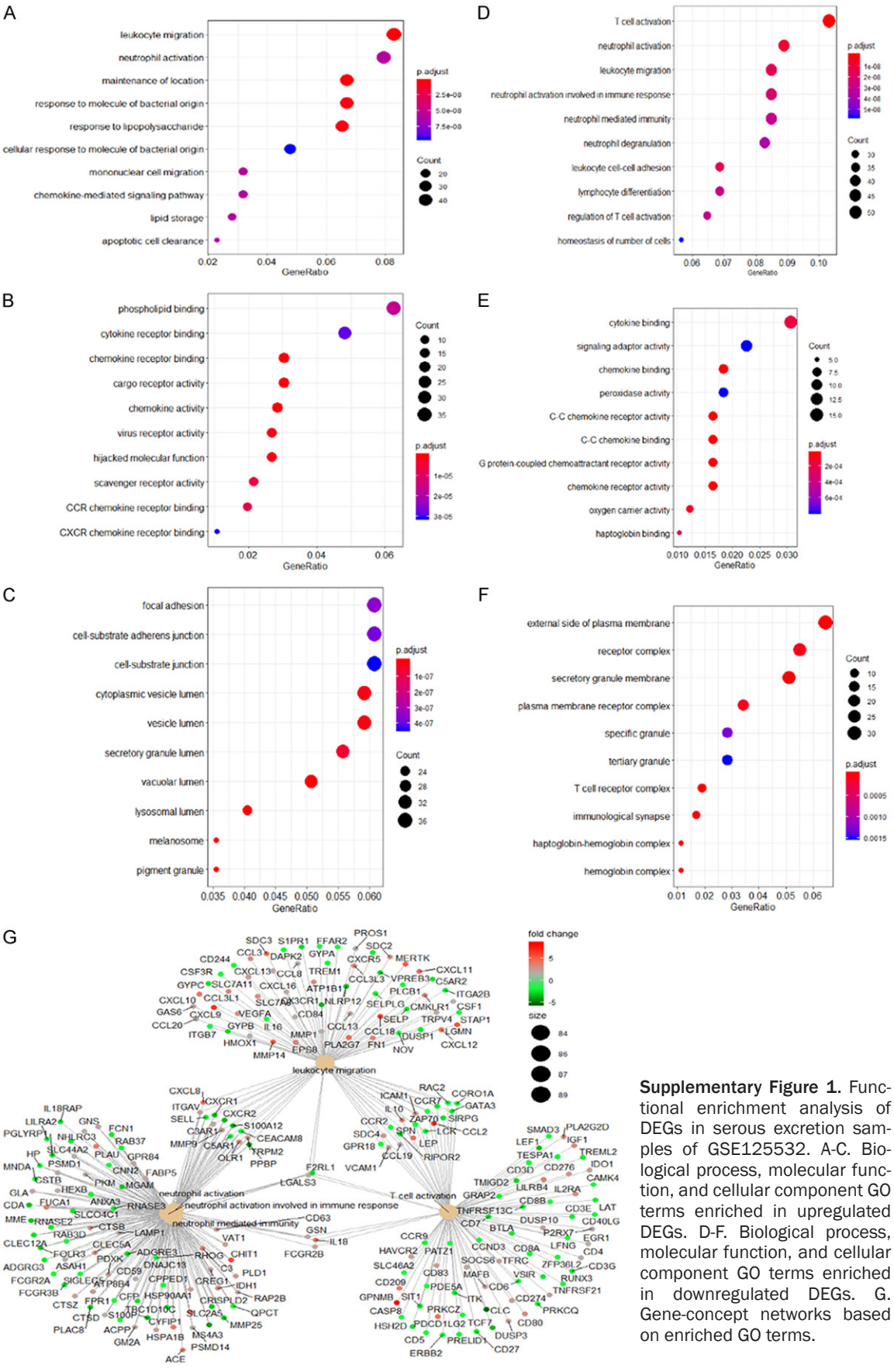

Supplementary Figure 1. Functional enrichment analysis of DEGs in serous excretion samples of GSE125532. A-C. Biological process, molecular function, and cellular component GO terms enriched in upregulated DEGs. D-F. Biological process, molecular function, and cellular component GO terms enriched in downregulated DEGs. G. Gene-concept networks based on enriched GO terms.

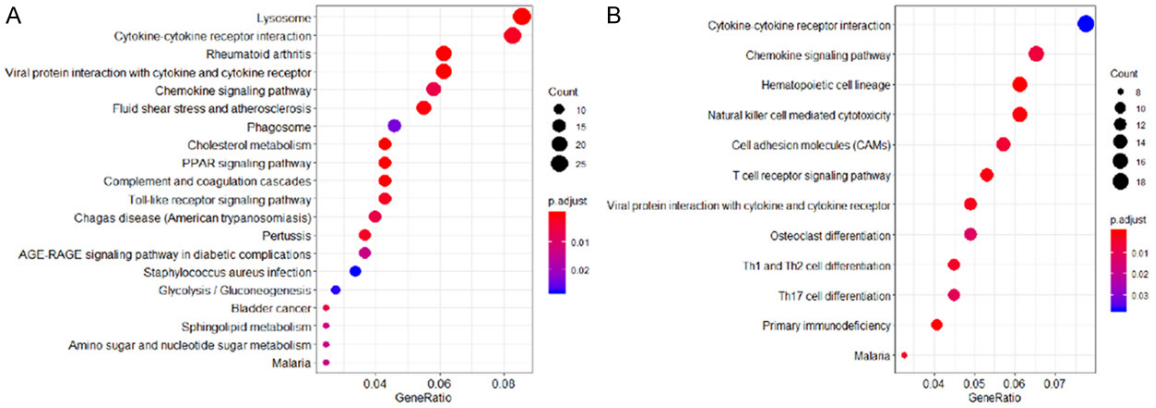

Supplementary Figure 2. KEGG enrichment analysis of DEGs in serous excretion samples of GSE125532. A. Upregulated. B. Downregulated.

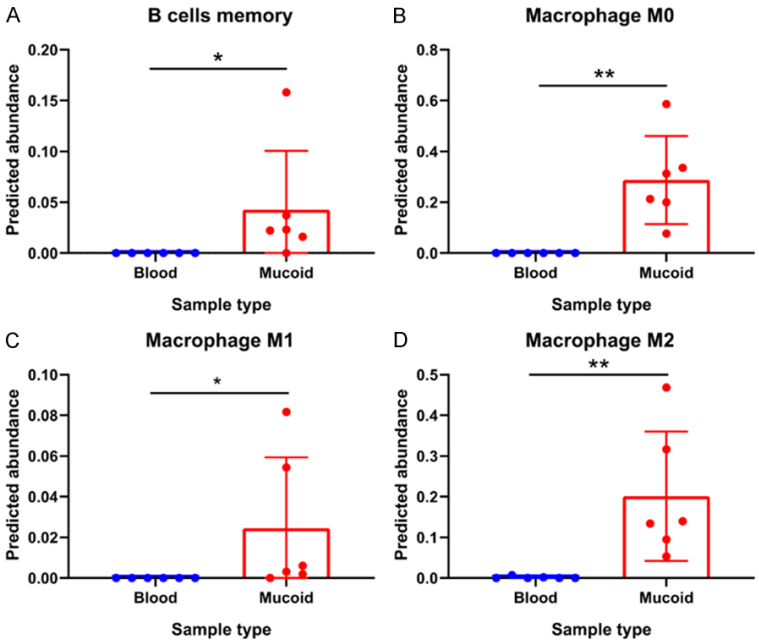

Supplementary Figure 3. FPKM based CIBERSORT predicted blood cell abundance between blood and mucoid excretion samples. Data are mean ± SE. *P<0.05, **P<0.01.

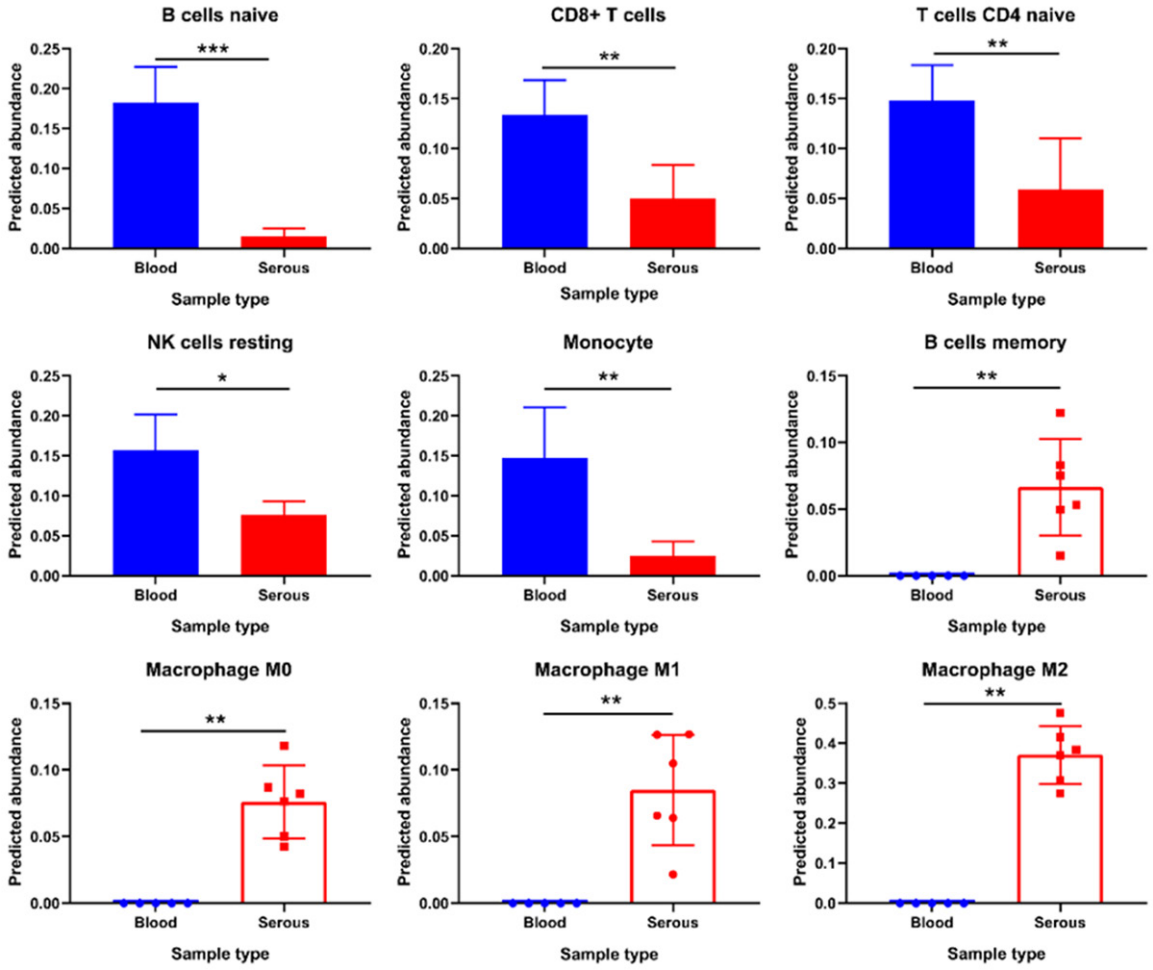

Supplementary Figure 4. FPKM based CIBERSORT predicted blood cell abundance between blood and serous excretion samples. Data are mean ± SE. *P<0.05, **P<0.01, ***P<0.001.

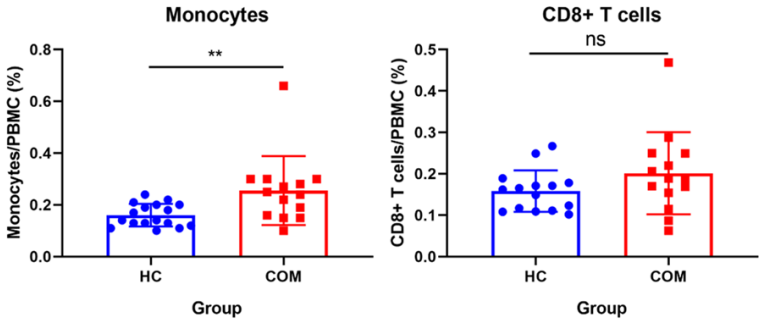

Supplementary Figure 5. Proportions of monocytes and CD8+ T cells in PBMC of the COM patients and HCs based on the blood routine data and the flow cytometry results, respectively. Data are mean ± SE. *P<0.05, ns: P≥0.05.